Presented and published through 13th International Heat Transfer Conference, Syndey, Australia, August 13-18, 2006

EXPERIMENTAL AND NUMERICAL CHARACTERIZATION OF TRANSIENT INSERTION OF HEAT FLUX GAGES IN A CYLINDRICAL BLACK BODY CAVITY AT 1100 °C

A. N. Abdelmessih[1], Ph.D., **T. Horn**[2]

[1]Saint Martin's University, 5300 Pacific Ave. S.E., Lacey, Washington 98503-1297, U.S.A.
[2]NASA, Dryden Flight Research Center, Edwards, California, U.S.A.

ABSTRACT

Initial transient thermal models have been developed to simulate a heat flux gage calibration process capable of generating high heat flux levels of interest to reciprocating and gas turbine engine industries as well as the aerospace industry. These transient models are based on existing, experimentally validated, steady state models of the cylindrical blackbody calibration system. The steady state models were modified to include insertion of a heat flux gage into the hot zone of the calibration system and time varying electrical current passing through the resistance heated blackbody. Heat fluxes computed using the initial transient models were compared to experimental measurements. The calculated and measured transient heat fluxes were within 5% indicating that the major physical phenomena in the transient calibration had been captured by the models. The predicted and measured transient heat fluxes were also compared at two different gage insertion depths. These results indicated that there is an optimum insertion position which maximizes heat flux and minimizes cavity disturbance.

NOMENCLATURE

T	=	temperature, °C
L	=	left cavity of the blackbody
R	=	right cavity of the blackbody
0-5	=	numerals 0 to 5 indicate time, where 0 is steady state, s

1. INTRODUCTION

High heat fluxes are generated within reciprocating engines, gas turbine engines, scramjet engines, and on the surfaces of hypersonic vehicles in flight. It is important to understand what these heat fluxes are in order to properly design hardware to survive these environments. Heat flux gages can be used to measure these heat fluxes but they need to be properly calibrated before they are put into service. In addition, the furnace used to calibrate these gages must be characterized in order to determine its effect on the accuracy of the calibration.

The National Institute of Standards and Technology (NIST) has made significant strides in recent years towards developing well understood calibration systems which operate in convection, conduction, and radiation heat transfer modes as reported by Holmberg, et al. (1997, 1999), Grosshandler and Blackburn (1997), and Murthy, et al (1997, 1999, 2000, 2001). The most powerful of the NIST facilities is a radiation facility from which they have reported heat flux calibrations up to 200 kW/m^2. This is below the heat fluxes which can be generated in hypersonic flight, which can be in excess of 1 MW/m^2. So far during calibrations NIST locates the heat flux gages outside the blackbody cavity at a distance safe enough not to create any disturbances to the thermal equilibrium of the blackbody.

The Flight Loads Laboratory (FLL) at the National Aeronautics and Space Administration's (NASA's) Dryden Flight Research Center is equipped with a calibration furnace capable of

calibrating heat flux gages above 1.3 MW/m^2 and temperature sensors up to 2200 ºC. This calibration system uses a cylindrical, dual cavity blackbody, for calibrating a reference heat flux gage. The calibration furnace manufacturer, Thermogage (1991), recommends that the blackbody temperature at the center of the middle partition be measured with a NIST traceable optical pyrometer and then the heat flux gage can be inserted into the blackbody cavity for a few seconds. The calibration of the heat flux gage is determined by dividing the emissive power of the blackbody by the peak output generated by the heat flux gage during the insertion. This process may be repeated at other temperatures, and hence heat fluxes, as required. This process of inserting the heat flux gage or any other measuring device affects the internal thermal equilibrium of the blackbody, creating transient conditions.

There are two key questions which must be answered in order to produce a quality heat flux gage calibration with well defined uncertainty intervals. First, what effect do the various boundary conditions such as conduction, radiation, convection, and the effect of axial temperature gradients have on the blackbody cavity as pointed out by Abdelmessih (1998, 1999), and Horn and Abdelmessih (2000). Second, what effect does the presence of the reference heat flux gage in the blackbody cavity have on the calibration? The measurement uncertainties associated with the later question have not been addressed in the literature and no detailed transient thermal analysis has been performed.

Research at the FLL aimed at quantifying the uncertainties associated with this calibration system and process has begun by performing experimental and numerical characterization of both the blackbody cavity under steady state conditions by Horn and Abdelmessih (2000), and under transient conditions to be discussed in this paper. Proper characterization of the system will require transient analyses of the reference heat flux gage insertion process.

This paper describes the detailed experimental measurements and transient thermal analysis made to characterize the transient conditions within the blackbody cavity during sensor insertion. It describes efforts to predict the nominal heat flux gage output during calibration and to identify and quantify calibration error sources

2. EXPERIMENTAL SET-UP

2.1 Test Setup

The calibration system, Figure 1, consists of a power supply, a dual cavity cylindrical blackbody, and an optical pyrometer for temperature control which views one side of the partition in the graphite tube. Other components not shown in Figure 1 include a computer used for data acquisition and temperature control, a cooling water system, and a supply of compressed argon gas.

The blackbody cavity (Figure 2a) is a hollow, 25.7 mm inside diameter, ATJ graphite cylinder 28.9cm long, with a 5.4 mm thick partition at the middle. At the top center of the graphite tube is an oval slot (Figure 2b) 9.4 mm long x 3.1 mm wide which serves as a bleed port for argon purge gas during pre-test purging of the blackbody cavities. The graphite tube is assembled with other components, shown in Figure 3. The graphite tube is held in place at each end by a graphite bushing assembly installed in a copper ring (Figure 3). A quartz tube, which serves as a containment barrier for argon purge gas, is held between the copper rings. The space between the outer surface of the blackbody and the quartz tube is insulated with graphite felt and foil when temperatures at 1100 °C or above are desired. The space is left uninsulated when the temperature does not exceed 1100 °C. Unheated graphite extension tubes, 15.2 cm long, are installed at both ends. Laminar flow of argon gas exiting the extension tubes prevents air from diffusing into the heated graphite tube.

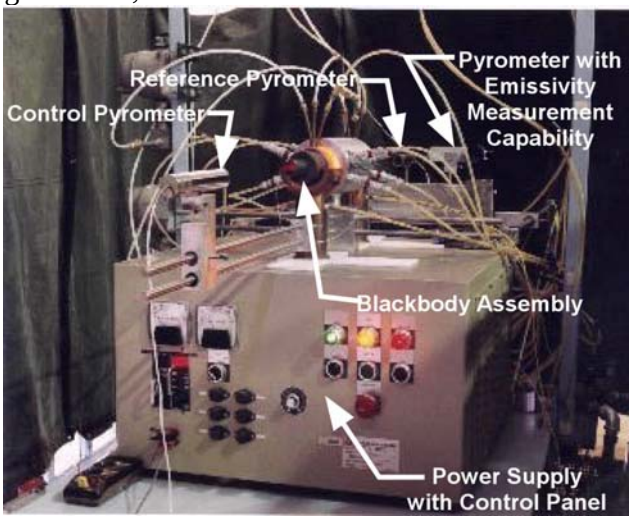

Figure 1: Blackbody calibration furnace.

a) Tube Overview

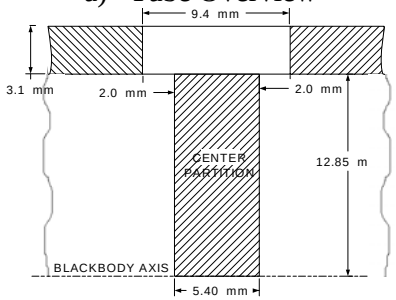

b) Partition Detail

Figure 2: Blackbody Tube.

Figure 3: Blackbody Assembly Components

.

This entire assembly is placed atop two electrodes (Figure 4) which are connected to the power supply. Stable temperatures between 800 °C and 2200 °C can be attained at the center of the graphite tube by passing regulated electric current from the power supply through the blackbody assembly. The copper electrodes and rings which hold the blackbody assembly are water cooled. An aluminum water cooled reflector (Figure 4) surrounds the quartz cylinder. This reflector serves as the radiation boundary for the external surface of the graphite tube during tests run without graphite insulation in the quartz cylinder.

Argon is used to purge the interior and exterior of the graphite tube to minimize/avoid oxidation of the graphite. Argon is introduced through ports in the copper rings at each end of the tube. Before heating, argon is forced into the blackbody cavity as well as the space between the graphite tube and quartz tube, including the insulation when installed. The location and geometrical configuration of the argon ports forces most of the argon to flow out the unheated extensions during the test run preventing oxygen from entering the hot graphite tube.

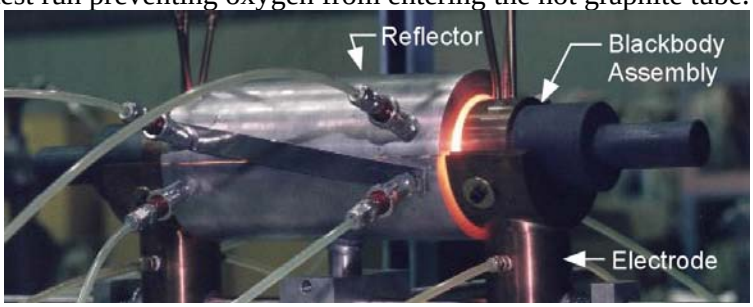

Figure 4: Assembled Blackbody on Electrodes.

The furnace temperature is computer controlled using the standard Proportional-Integral-Derivative algorithm in a commercial data acquisition and control software package. An optical pyrometer views the center of the mid-partition from one end of the blackbody and provides temperature feedback to the control system. The thermal control system maintains the indicated temperature within ±0.5 °C of the desired steady state set point from 800 °C to 2200 °C.

2.2 Instrumentation

Various measurements were required to characterize the blackbody cavity. They include the temperature at the center of the partition in the middle of the blackbody, partition emissivity, electrical current passing through the blackbody assembly, axial blackbody heat flux profiles, and location of the axial heat flux sensor.

2.2.1 Optical Pyrometers: Three optical pyrometers (Figure 1) were utilized during the experimental characterization of the blackbody cavity. The control pyrometer and reference pyrometer measured blackbody temperature. These pyrometers were identical radiation pyrometers for measuring temperatures between 800 °C and 3100 °C. Their measurement spot covers approximately ¼ of the diameter of the blackbody partition. The control pyrometer provides feedback to the control system to maintain stable temperatures. The reference pyrometer was calibrated at NIST prior to testing with a 95% confidence uncertainty of 0.7 °C at 1100 °C. The temperature measurements of the center partition with the reference pyrometer will be referred to as the blackbody temperature throughout this paper. The third pyrometer included a system for measuring surface emissivity, at both room temperature and test temperatures. The data from this pyrometer was used in the original development of the steady state thermal models as described in Horn and Abdelmessih (2000).

2.2.2 Heat Flux Gage: A circular foil (Gardon) heat flux gage was used. The heat flux gage is approximately 13 mm in diameter and is situated at the end of a 50.1 cm long water cooled probe. The manufacturer's calibration was used to convert the heat flux gage output to engineering units reported in this paper.

2.2.3 Heat Flux Gage Position Measurement: The position of the heat flux gage sensing tip was measured using a deflection measurement potentiometer. The range of the device was 0 to 1080mm. The measurement system was calibrated such that 0 mm was indicated with the surface of the measuring instrument in contact with the center partition.

2.2.4 Electric Current Measurement: The electrical current passing through the blackbody assembly was measured using a current transformer and current transducer, which converted the current to direct current (DC) voltage. This DC voltage could then be acquired by the data acquisition system.

2.2.5 Measurement Uncertainty: The total (sensor and data acquisition) uncertainties at 1100 °C for the pyrometers, current, emmisivity, and axial location were quantified to be 0.7 °C, 1.3 A, 0.01, 1.6 mm, respectively. Uncertainties for the various measurements are described in Horn and Abdelmessih (2000).

2.3 Test Procedure

The process of configuring the calibration system for test and establishing the test temperature in the blackbody is described in detail in Horn and Abdelmessih (2000). The blackbody was installed in either the insulated or uninsulated configuration, cooling water flow and argon purge (argon flow at 0.28 m^3/hr) was established, and the blackbody was heated and stabilized at 1100° C. The temperature of 1100 ºC was chosen because it is the temperature at which the heat flux calibration system manufacturer recommends switching from the uninsulated blackbody configuration used at lower temperatures to the insulated configuration used at higher temperatures. Thus allowing a comparison between the effect of different boundary conditions at 1100 °C.

Once the blackbody temperature was stabilized according to the control pyrometer, the blackbody temperature was checked with the NIST calibrated reference pyrometer. These temperatures were

measured on opposite sides of the center partition and were within ±0.4 °C, within the uncertainty of the NIST pyrometer calibration. The NIST calibrated pyrometer was then moved away from the blackbody axis in order to provide a clear view for the infrared pyrometer and the emissivity measurement was taken.

Once the emissivity measurement was recorded, the heat flux gage was positioned in front of the blackbody. The heat flux gage was then plunged (<1 second of motion) into the blackbody while its tip location, heat flux measurement, and cooling water to the gage were recorded by the data acquisition system. The slide track, on which the heat flux gage was mounted, was pushed against a stop for the full insertion at 4 mm and this axial position was repeated within the measurement uncertainty previously stated. The sensor was left at maximum depth for approximately 6 seconds and then pulled out of the blackbody.

3. TRANSIENT THERMAL ANALYSIS

Numerical transient thermal analyses of the insulated and uninsulated blackbody configurations were developed to help in understanding the relevant heat transfer mechanisms occurring during the calibration process. The steady state models of the blackbody developed by Horn and Abdelmessih (2000) formed the basis of the transient models. The external radiation and contact boundary conditions remained unchanged from the steady state work as did the geometry, mesh, and various material properties used. These details will not be discussed extensively here. This work includes the insertion of the heat flux sensor in the cavity and the time varying electric current utilized in the heat generation calculation.

3.1 Software

Numerical models of the blackbody assembly were developed, for both the insulated and uninsulated configurations, using commercially available thermal analysis software by MacNeal-Schwendler Corporation (2005). The software includes a user interface for model generation and a radiation view factor analysis program in addition to a finite element method based thermal solver.

3.2 Geometry and Grid

The numerical model geometry, as developed for the previous steady state work (2000), is a two-dimensional cross section, bounded by the centerline axis and included both cavities of the blackbody assembly. The graphite tube, end cap bushings, and extensions were fully modeled. Options selected in the thermal analysis software instruct the solver to interpret the geometry as a thin slice of an axisymmetric object and compute the radiation and conduction heat transfer accordingly.

The heat flux gage was modeled as a constant temperature surface using bar elements, 2 mm mesh. This model was stationary in the blackbody cavity resulting in an assumption that the temperature distribution in the blackbody did not change significantly during the rapid insertion of the heat flux gage during test.

The node spacing in the blackbody wall was nominally 2 mm axial by 1 mm radial, see Figure 6 below. Details of the blackbody mesh are described in Horn and Abdelmessih (2000).

3.2.1 Insulated Model: Graphite felt surrounds the blackbody tube in the insulated configuration but was not included in the model geometry, see Figures 5a and 6. The effect of the insulation was modeled as an adiabatic boundary condition on the exterior tube wall and reduced current passing through the graphite tube, as discussed below.

3.2.2 Uninsulated Model: The water cooled copper ring at each end cap and the water cooled aluminum reflector were represented as surfaces at fixed temperatures for the uninsulated model geometry and mesh. The copper caps and aluminum reflector were included as boundaries in the model to properly define the radiant heat transfer from the external surface of the uninsulated graphite tube.

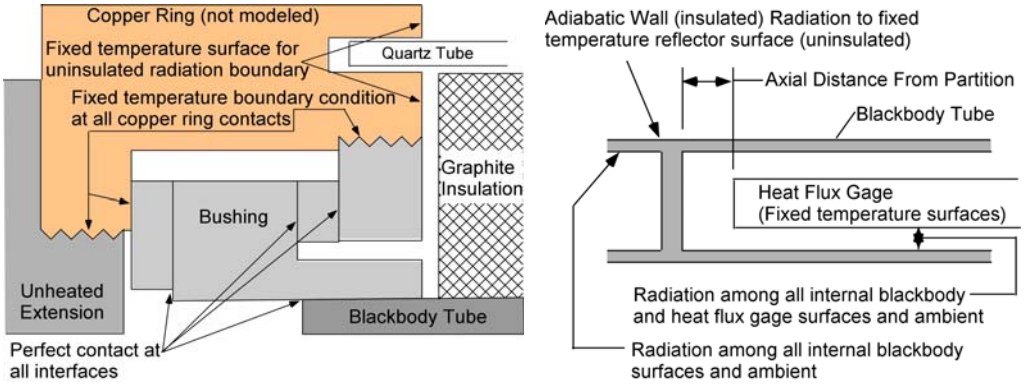

Figure 5: Thermal Model Boundary conditions for: (a) the bushing geometry (left) and, (b) blackbody tube with heat flux gage inserted (right)

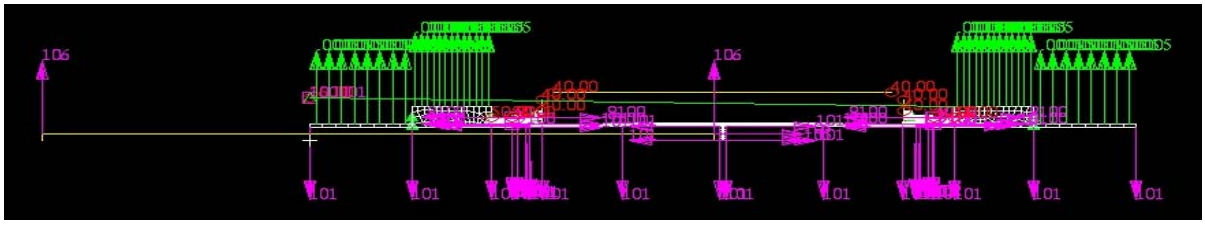

Figure 6: Boundary conditions on the patran insulated blackbody with the heat flux gage inserted 4mm from the center partition in the left cavity

3.3 Modeling Assumptions

3.3.1 Thermal Contact Resistance: Thermal contact resistance, though significant in the actual hardware, was neglected in this analysis. The boundary temperatures at the end caps were used in the steady state analysis as a tuning parameter to match the calculated blackbody temperature profile to test data. These temperature boundary conditions were unchanged in the transient analysis.

3.3.2 Blackbody Cavity Internal Convection: Convection inside the blackbody cavity was found to be negligible, by Abdelmessih (1998, 1999). The argon flow rate input at each end cap was $0.14 m^3/hr$, for all runs. Due to a lack of resistance to flow, the majority of the argon exits through the extension tubes, i.e. forced convection is not expected to be significant in the blackbody cavity. It is assumed that natural convection will not significantly alter the blackbody temperature distribution during the short time that the heat flux gage is inserted.

3.4 Heat Generation

Heat was input into the insulated and uninsulated thermal models via volumetric heat generation. The thermal solver computed the heat generation per unit volume based on the actual total current passing through the blackbody assembly, the local geometry of the assembly, and the electrical resistivity. The models included temperature dependent electrical resistivity for the ATJ graphite tube and constant electrical resistivity for the pyrolytic graphite and carbon-carbon components. The reader should refer to Horn and Abdelmessih (2000) for the details of this calculation.

The total electric current passing through the assembly was measured during each test and the measured value was used in the model. The model includes time varying current as measured during each heat flux gage plunge beginning with first motion of the heat flux gage.

3.5 Boundary Conditions

The boundary conditions on the external surfaces of the blackbody, including radiation (uninsulated,) adiabatic wall (insulated,) and contact temperature, were symmetric about the center partition. The internal boundary conditions were asymmetric about the partition due to the presence of the heat flux gage on one side. The external boundary conditions and those in the empty cavity were thoroughly described in Horn and Abdelmessih (2000).

Unique boundary conditions existed on the external surface of the blackbody tube for uninsulated and insulated configurations. The model of the uninsulated configuration included radiation exchange between the blackbody tube and the water cooled copper rings and aluminum reflector. The adiabatic wall boundary condition on the external surface of the blackbody tube was used for the insulated model.

3.5.1 Bushing/Copper Ring Boundary Temperature: A fixed isothermal temperature boundary condition was enforced at the points where the bushings contacted the copper rings in each end cap. Figure 5a. These temperatures were fixed according to the steady state models developed by Horn and Abdelmessih (2000).

3.5.2 Heat flux gage: The cylindrical body of the heat flux gage is oxidized brass had an emmisivity of 0.6, in agreement with values reported by Seigel and Howel (1992). The face of the heat flux gage is painted with a flat black paint having an emmisivity of 0.9. Both the body and face were set at a fixed temperature. The fixed temperature was chosen as the experimentally measured water temperature passing through the heat flux gage. Figures 5b and 6 show the heat flux gage inserted in the blackbody cavity.

3.5.3 Initial temperature of the blackbody: The nodal temperatures of the steady state blackbody model , as reported by Horn and Abdelmessih (2000), were reproduced and used as the initial nodal temperatures for each of the transient models.

3.5.4 External Surface Radiation from the Blackbody Tube (Uninsulated Blackbody): Radiation exchange was included in the uninsulated model between the exterior of the blackbody and the copper rings and aluminum reflector. The same emissivity values used by Horn and Abdelmessih (2000) for the copper rings and aluminum reflector were used in the transient models. Both the copper and aluminum surfaces had significant surface oxidation. Ring and reflector emissivities of 0.26 were used, see Table 1.

3.5.5 Adiabatic Wall (Insulated Blackbody): The adiabatic wall boundary condition was enforced on the exterior of the graphite tube in the model of the insulated configuration. An insignificant amount of heat was expected to flow radially through the insulation due to the thermal resistance of the insulation and the heating of the insulation by a portion of the electric current passing through the blackbody assembly.

3.6 Material Properties

Thermal conductivity and electrical resistivity for ATJ graphite were available from the manufacturer as a function of temperature throughout the range of interest. Values for the thermal conductivity and electrical resistivity of pyrolytic graphite at room temperature were obtained from Clauser et al (1963). Extensive coverage of material properties is given by Horn and Abdelmessih (2000). The emissivity of the ATJ blackbody center partition was measured as part of the test and

was used as the emissivity for all graphite radiating surfaces. Published values by Siegel and Howell (1992) were used for initial estimates for the aluminum reflector and copper ring emissivity (Table 1). The copper and aluminum emissivities are heavily dependent on the degree of oxidation so they are used only as a guide. Measurement of the highly specular copper and aluminum emissivities was not possible since the available emissivity measuring equipment required diffuse reflection for proper operation.

Table 1: Material Emissivity

Material	**ATJ Graphite** (measured, used for all graphite components)	**Oxidized Aluminum** Siegel and Howell, (1992)	**Copper** (depending on level of polish and oxidation) Siegel and Howell (1992)
Emissivity	0.88 – 0.91	0.20 – 0.31	0.15 - 0.78

4. RESULTS

Two transient models were developed. The blackbody is uninsulated in the first model and represents the calibration system configuration at temperatures of 1100 °C or less. The second model represented the blackbody insulated with graphite felt for use at temperatures at or above 1100 °C. The blackbody transient models used the blackbody geometry and mesh from the steady state models reported by Horn and Abdelmessih (2000). Simple heat flux gage models were added to one cavity in each of the models with surface properties and temperature as described above.

The steady state models reported by Horn and Abdelmessih (2000) were rerun to verify the results generated by the latest version of the analysis software. Figures 7 and 8 show the steady state temperature profiles in the blackbody cavities along the axis of the insulated (parabolic heat generation temperature profile) and uninsulated (radiation losses flattens the temperature profile) models, respectively, as generated by the latest software version. The modeled temperature profiles are exact duplications of the steady state models by Horn and Abdelmessih (2000), who compared the models with experimental measurements reported by Abdelmessih (1998) and found both models and experimental results in agreement.

Experimentally, the maximum insertion of the heat flux gage in the blackbody cavity was 4 mm from the center partition Abdelmessih (1998). This maximum insertion would have the maximum effect on the blackbody temperature. Figure 9 shows the experimental reading of the heat flux gage (pink) as a function of time (x-axis) and heat flux gage distance from the partition (dark blue) in the blackbody.

4.1 Uninsulated transient models

For the first step in the development of the transient model the fixed temperature surfaces representing the heat flux gage were added. The motion of the heat flux gage during the plunge was not modeled, depicting an instantaneous insertion of the gage. Preliminarily, the transient analysis was run with the same fixed electrical current as the steady state models, to verify that the radiant exchange between the heat flux gage surfaces and the blackbody surfaces was working properly.

Time varying electrical current was then added to the transient model heat generation calculation to account for the reaction of the temperature feedback control system to the cooling of the blackbody after heat flux gage insertion. Figure 10 shows the experimental current measurement during a heat flux gage plunge. Figures 11 and 12 show the calculated transient temperature of the cavity and partition, respectively, due to the insertion of the heat flux gage in the left cavity and time varying current. The calculated temperatures seem reasonable given the time history of the experimental heat flux gage output as shown in Figure 9. The heat flux gage output peaks and decreases slightly

during the final stages of the plunge, consistent with the initial cooling of the blackbody. The step features in the heat flux gage output may represent the effect of the purge gas slot in the wall of the blackbody at the center partition. This slot was not modeled.

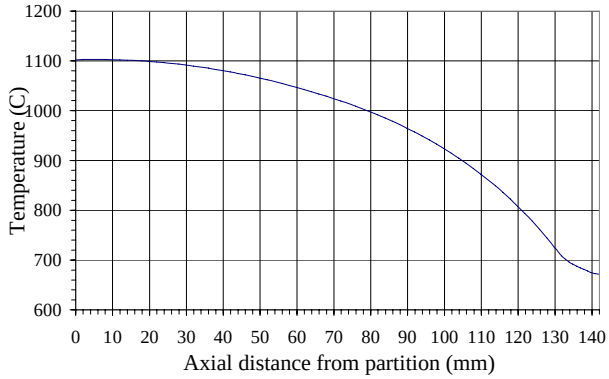

Figure 7: Numerically calculated temperature profile for the steady state left cavity of the insulated blackbody.

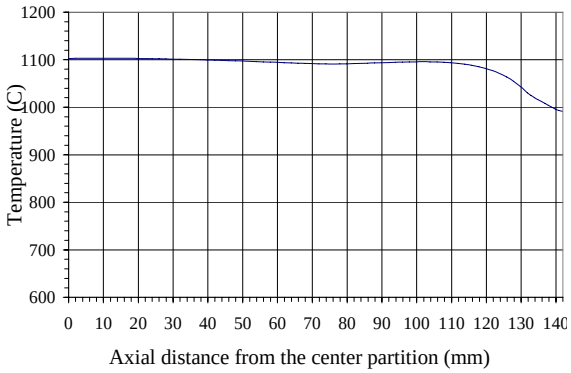

Figure 8: Numerically calculated temperature profile for the steady state left cavity of the uninsulated blackbody

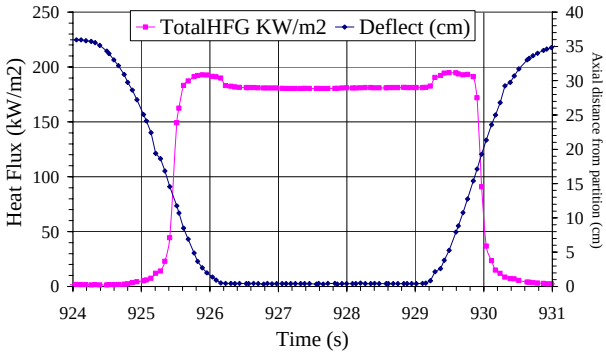

Figure 9: Heat flux gage inserted up to 4 mm from the center partition of an uninsulated blackbody at 1100 °C.

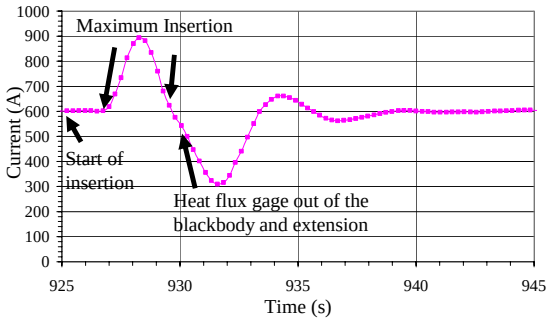

Figure 10: Fluctuations in current due to the insertion of the heat flux gage to a depth of 4 mm from the center partition of the uninsulated blackbody cavity.

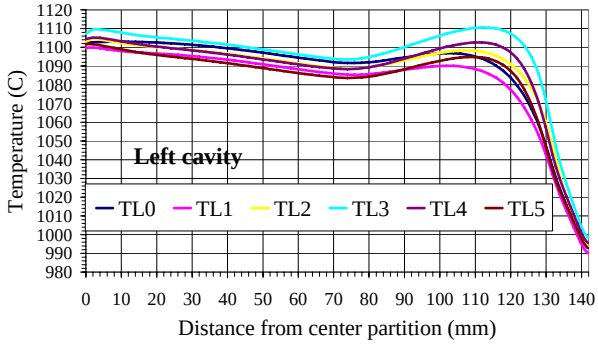

Figure 11: Insertion of the heat flux gage in the uninsulated blackbody to a depth of 4 mm from the center partition in the left cavity, accounting for the fluctuations in the current.

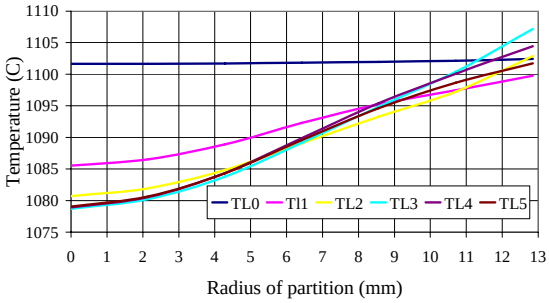

Figure 12: Variation of temperature in the center partition of the uninsulated blackbody due to the insertion of the heat flux gage to a distance of 4 mm from the center partition, accounting for the variation in current.

The measured heat flux (Figure 9) remains remarkably constant while the gage remains in the blackbody. An estimate of the incident heat flux at the face of the gage was generated using the correlation by Leuenberger and Person (1956) for a disk in a cylinder. The measured and estimated heat fluxes are tabulated in Table 2. Comparison of the measured and estimated heat fluxes indicate that the transient thermal model captures the trends of the experimental data and agrees with the

heat flux indicated by the gage within about 3% for an insertion depth of 4 mm, uninsulated. This indicates that the simple model of the heat flux gage insertion process has captured the most significant aspects of the physical problem.

The potential effect of the purge gas slot may be minimized by maintaining a greater distance between the blackbody partition and the heat flux gage face. Figure 13 shows the measured heat flux and position time histories for a heat flux gage insertion to a point 14.3 mm from the blackbody partition. This heat flux time history lacks the step features visible in Figure 9. Figures 14 and 15 show the variations in axial temperature and partition temperature in the left cavity where the heat flux is inserted, respectively. Table 2 also includes the measured and estimated heat fluxes for this insertion depth. This data also shows the proper trends being captured and about a 4% difference in magnitude.

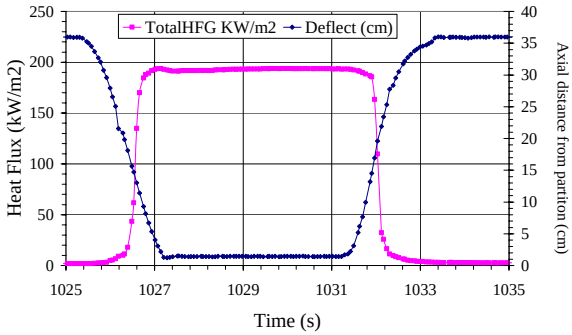

Figure 13: Heat flux gage inserted up to 14.3mm from the center partition of the blackbody at 1100 °C.

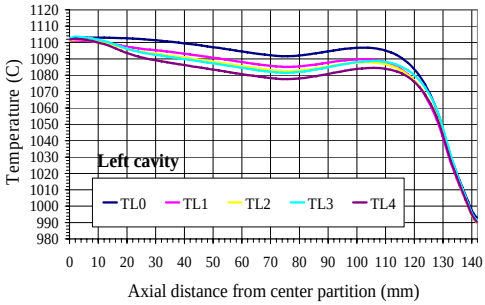

Figure 14: Insertion of the heat flux gage to a depth of 14.3 mm in the left cavity of the uninsulated blackbody, accounting for variation in current.

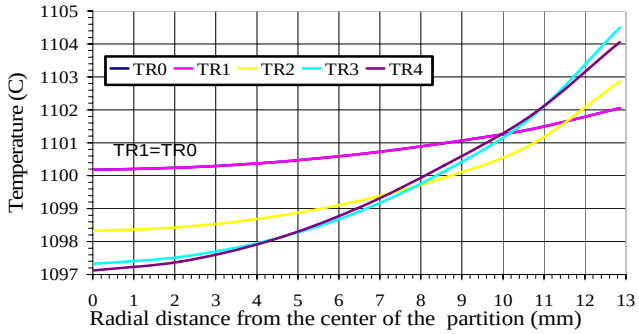

Figure 15: Effect of the heat flux insertion to a depth of 14.3 mm from the partition, right partition wall temperature

4.2 Insulated transient model

For the insulated transient model only the extreme case of maximum insertion of the heat flux gage to a depth of 4 mm from the center partition has been completed. The measured variations of the electric current are included in the model. Figures 16 and 17 show the predicted effect of insertion of the heat flux gage on the temperature of the blackbody cavities and partition, respectively. The measured and estimated heat fluxes for this model are also shown in Table 2. Again, the trends are captured and there is about 4% difference between the measured and estimated heat fluxes. This indicates that the insulated model also captures the most significant physics of the problem.

5. CONCLUSION

Initial transient models of a heat flux gage calibration process have been developed. This process involves the insertion of a cooled heat flux gage into a blackbody cavity in order to achieve higher heat flux levels. The transient models were developed for the blackbody at a nominal 1100° C in

insulated and uninsulated configurations. Comparison of indicated output of a heat flux gage and incident heat flux estimates derived from transient thermal model temperature distributions indicate that the current models capture the most significant aspects of the gage insertion problem. Measured and calculated heat fluxes followed the same trends with insertion time and position and were within 5% of each other.

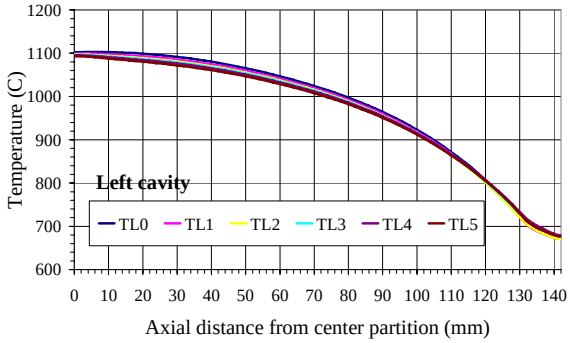

Figure 16: Heat flux gage transient insertion to 4 mm from the partition in the left cavity of an insulated blackbody.

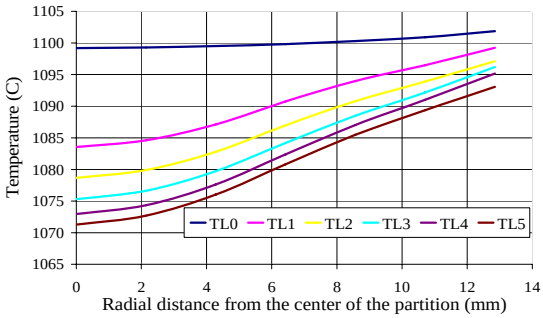

Figure 17: Variation of temperature in the left center partition of the insulated blackbody due to the insertion of the heat flux gage..

Table 2: Comparison of experimentally measured heat fluxes with predicted heat fluxes, as a function of time for the three models.

Model	Time (s)	Measured (kW/m2)	Predicted (kW/m2)
Uninsulated (4mm)	1	182.3	176.9
	2	180.3	176.2
	3	181.2	176.8
Uninsulated (14mm)	1	192.9	186.0
	2	192.9	185.8
	3	192.0	186.2
	4	193.2	185.7
Insulated (4mm)	1	181.2	176.2
	2	180.3	174.4
	3	180.3	173.2

The results derived from both experimental measurements and the thermal models indicate that there is an optimum insertion depth which minimizes the disturbance to the blackbody (and hence calibration error) and maximizes incident heat flux on the gage. Additional work is still required to identify the optimum location and quantify the measurement uncertainty. Also more experiments and modeling should be performed for a black body cavity with a larger diameter over a temperature range from 800 °C to 1900 °C.

6. ACKNOWLEDGMENT

This work was performed as part of the NASA Summer Faculty Research Program. The experiments were performed in the Flights Loads Laboratory, at NASA's Dryden Flight Research Center, Edwards, California. Thanks are due to the Flight Loads Laboratory.

7. REFERENCES

Presented and published through 13th International Heat Transfer Conference, Syndey, Australia, August 13-18, 2006
Abdelmessih, A. N., 1999, "Analysis of Cylindrical Blackbody," NASA Technical Reports, NGT 2-52212, Document ID, PP A:1-4.

Abdelmessih, A. N., 1998, "Experimental Measurements of Temperature and Heat Flux in a High Temperature Black Body Cavity," NASA Technical Reports, NGT 2-52212, Document ID 19990021026, PP A:1-3.

Clauser, H. R., Fabian, R., Peckner, D., and Riley, M. W., 1963, "The Encyclopedia of Engineering Materials and Processes", Reinhold Publishing Corp., New York, NY.

Grosshandler, W. L,. and Blackburn, D., 1997, "Development of a High Flux Conduction Calibration Apparatus," HTD-Vol. 353, *Proceedings of the ASME Heat Transfer Division, V. 3*, pp 153 – 158.

Holmberg, D., Steckler, K,. Womeldorf, C,. and Grosshandler, W., 1997, "Facility for Calibrating Heat Flux Sensors in a Convective Environment," HTD-Vol. 353, *Proceedings of the ASME Heat Transfer Division, V. 3*, pp 165 – 171.

Holmberg, D. G., Womeldorf, C. A., and Grosshandler, W. L., 1999, "Design and Uncertainty Analysis of a Second-Generation Convective Heat Flux Calibration Facility," HTD-Vol. 364, *Proceedings of the ASME Heat Transfer Division, V. 4*, pp. 65 – 70.

Horn, T., and Abdelmessih, A. N., August, 2000, "Experimental and Numerical Characterization of Steady State Cylindrical Blackbody Cavity at 1100 °C," Proceedings of the *34th National Heat Transfer Conference*, Pittsburgh, U.S.A..

Leuenberger, H., and Person, R. A., 1956, "Compilation of Radiation Shape Factors for Cylindrical Assemblies," *proceedings of the ASME annual meeting, 56-A-144, New York.*

MacNeal-Schwendler Corporation, 2003, MSC/PATRAN THERMAL Users Guide, Volumes 1 and 2. Software Version is Patran2005.

Murthy, A. V., Tsai, B. K., and Saunders, R. D., 1997, "Radiative Calibration of Heat Flux Sensors at NIST – An Overview," HTD-Vol. 353, *Proceedings of the ASME Heat Transfer Division, V. 3*, pp 159 - 164.

Murthy, A. V., Tsai, B. K., and Saunders, R. D., 1999, "Comparitive Calibration of Heat Flux Sensors in Two Blackbody Facilities," *J. Res. Natl. Inst. Stand. Technol., V. 104, Number 5,* pp 487 - 494.

Murthy, A. V., Tsai, B. K., and Saunders, R. D., 2000, "Radiative Calibration of Heat-Flux Sensors at NIST: Facilities and Techniques," *J. Res. Natl. Inst. Stand. Technol., V. 105, Number 2,* pp 293 - 305.

Murthy, A. V., Tsai, B. K., and Saunders, R. D., 2001, "Transfer Calibration Validation Tests on a Heat Flux Sensor in The 51 mm High-Temperature Blackbody," *J. Res. Natl. Inst. Stand. Technol., V. 106, Number 5,* pp 823 - 831.

Siegel, R., and. Howell, J. R., 1992, Thermal Radiation Heat Transfer, 3rd edition, Hemisphere Publishing Corporation, Washington, D.C.

Presented and published through 13th International Heat Transfer Conference, Syndey, Australia, August 13-18, 2006
Thermogage Inc., 1991, “Thermogage Operation Manual for Model 48 kW Calibration Furnace,” Forstburg, Maryland.